*Fibers and Polymers* 2007, Vol.8, No.3, 271-277

# Metal Ion Adsorbability of Electrospun Wool Keratose/Silk Fibroin Blend Nanofiber Mats

**Doo Hyun Baek[1], Chang Seok Ki[1], In Chul Um[2], and Young Hwan Park[1,3]***

[1]*Department of Biosystems and Biomaterials Science and Engineering, Seoul National University, Seoul 151-742, Korea*
[2]*Department of Natural Fiber Sciences, Kyungpook National University, Daegu 702-701, Korea*
[3]*Research Institute for Agriculture and Life Science, Seoul National University, Seoul 151-742, Korea*
(Received February 26, 2007; Revised April 11, 2007; Accepted April 13, 2007)

**Abstract:** In this study, electrospun wool keratose (WK)/silk fibroin (SF) blend nanofiber was prepared and evaluated as a heavy metal ion adsorbent which can be used in water purification field. The WK, which was a soluble fraction of oxidized wool keratin fiber, was blended with SF in formic acid. The electrospinnability was greatly improved with an increase of SF content. The structure and properties of WK/SF blend nanofibers were investigated by SEM, FTIR, DMTA and tensile test. Among various WK/SF blend ratios, 50/50 blend nanofiber showed an excellent mechanical property. It might be due to some physical interaction between SF and WK molecules although FTIR result did not show any evidence of molecular miscibility. As a result of metal ion adsorption test, WK/SF blend nanofiber mats exhibited high $Cu^{2+}$ adsorption capacity compared with ordinary wool sliver at pH 8.5. It might be due to large specific surface area of nanofiber mat as well as numerous functional groups of WK. Consequently, the WK/SF blend nanofiber mats can be a promising candidate as metal ion adsorption filter.

**Keywords:** Wool keratose, Silk fibroin, Nanofiber, Metal ion, Adsorption

## Introduction

It has always been an issue how heavy metals ions, such as mercury, lead, copper, nickel and cadmium, can be efficiently removed in waste water because an effluent in various industries such as dyeing, plating, painting, electronics, etc. and can cause crucial health problems on human body and environment. However, it is very difficult to exclude the toxic metal ions from aqueous solution with general water treatment methods. Therefore, a wide variety of removal methods have been proposed such as precipitation, coagulation/flocculation, cementation, chelation and ion exchange although these techniques either have the inherent problem of sludge handling and disposal and/or are best suited for solutions having high metal concentrations [1]. Besides, these materials for conventional water treatment are somewhat expensive and the treatment requires complex operational set-up. Accordingly, an alternative method makes a demand for removing heavy metal ion and adsorption technique using cheap materials like agricultural product have been suggested.

Especially, wool keratin fiber can be a candidate as metal ion adsorbent because it has numerous polar and ionizable groups on the side chain which can bind charged metal ions in water [2]. Furthermore, if waste wool fibers are used, they have much benefit for low cost and recycling of waste material. Therefore, many researchers have been investigating about metal ions adsorption capacity of wool protein [3-6].

Electrospinning is a method to fabricate ultrafine fiber of nanometer scale by using electric potential. Compared with conventional fiber spinning, this method does not require complex equipments. Generally, electrospinning apparatus is composed of high DC voltage power supply, collecting plate or drum and dope flow rate controller. Moreover, it has a great versatility for spinning polymers, even inorganic compounds. The diameter of electrospun nanofiber can be easily control in a certain range by spinning conditions such as dope concentration, applied voltage and additive.

A remarkable characteristic of electrospun nanofiber is a huge surface area for unit mass, which yields many profitable properties. For textiles, light and smooth fabric can be made. And, it can be adopted as an adsorption air filter [7,8], high performance electrode [9], drug delivery substrate [10,11], cell culture matrix [12-16], sensor [17-19] and support for enzyme immobilization [20,21] based on its large surface area.

In this study, we focused on the water permeation filter of wool and silk protein for metal ion adsorption. This attempt is to bind two advantages of the metal ion adsorption ability of wool and large surface area of electrospun nanofibers for developing a novel material with high performance as metal ion absorbent. For electrospinning, the wool keratin was converted to keratose, known as a soluble derivative of keratin, by a cleavage of disulfide bonds. However, based on our preliminary experiment, wool keratose (WK) has exhibited poor electrospinnability and morphological instability in water due to a low molecular weight caused in oxidation process and difficulty to handle because of brittleness. Therefore, the dope solution was prepared by blending WK and silk fibroin (SF). It has been reported that the SF is easily electrospun into nanofiber and excellent shape stability in aqueous solution. Furthermore, it is well known that the SF also has an adsorption capacity of metal ions [22-26]. Therefore,

*Corresponding author: nfchempf@snu.ac.kr

the electrospun WK/SF blend nanofiber mats was prepared and characterized for evaluating the potential of these nanofibers as a metal ion absorbent using copper (II) ion.

## Experimental

### Materials

The scoured Merino wool fiber was immersed in performic acid of 1:30 liquor ratio at 0 °C for 24 h. The performic acid was prepared by mixing 98 % formic acid (Kanto, Japan) and 30 % hydrogen peroxide (DC Chemical, Korea) for an hour at room temperature. Then, the soluble fraction of oxidized wool fiber was filtered and dried at ambient temperature.

For obtaining silk fibroin, *Bombyx mori* cocoons were boiled with an aqueous solution of marseillus soap 0.3 wt.% and sodium carbonate 0.2 wt.% at 100 °C for an hour to remove sericin. Then the SF fibers were rinsed thoroughly in warm distilled water and dried. The degummed SF fibers were dissolved in a ternary solvent system of $CaCl_2/H_2O$/EtOH (mole ratio=1/8/2) solution at 85 °C for 15 min and dialyzed to remove salts in cellulose tube (MWCO: 12,000-14,000) against distilled water for 3 days at room temperature. And the aqueous SF solution was freeze-dried.

### Electrospinning

For the preparation of dope solution, the WK and SF were dissolved in 98 % formic acid with various blend ratios (WK/SF: 100/0, 90/10, 70/30, 50/50, 30/70, 10/90, 0/100) for 4 hours at room temperature. The solution was filtered to remove impurities. Then, each dope solution was placed in a syringe of 10 m*l* with stainless steel syringe needle (22 G, inner diameter: 0.4 mm) as an electrode. The syringe was loaded in a syringe pump (KD Scientific, USA) to control a flow rate accurately with spinning rate. The syringe needle was connected to power supply (Chungpa EMT High Voltage Supply, Korea). Rolling stainless drum was used as a collector for obtaining sheet type nanofiber assemblies and grounded. The flow rate of dope solution was controlled to maintain a constant size of droplet at the tip of the syringe needle. The electrospinning condition was performed at room temperature and 60 % relative humidity. Electric potential and distance to collector were fixed at 15 kV and 10 cm, respectively.

### Characterization

For structural and mechanical measurement, the electrospun blend nanofiber mats were treated with methanol by soaking in the bath for the crystallization of SF. Morphological structure of the blend nanofibers was examined using scanning electron microscopy (SEM) (JSM-5410LV, JEOL, Japan) and the obtained images were analyzed by image analyzing software (ImagePro, USA). The conformation of the blend nanofiber mats was analyzed by FTIR spectrometer (M series, MIDAC corporation, USA) in the scanning range of 4,000-400 $cm^{-1}$. To evaluate the miscibility of WK/SF blend, blend films were prepared and analyzed by dynamic mechanical thermal analyzer (DMTA MARK IV, Rheometric Scientific, UK) at 4 scanning rate, 30-280 °C temperature, 0.5 Hz frequency and 0.1 % strain. Tensile properties of nanofiber mats were measured by tensile tester (MINIMAT, TA instrument, USA). Ten specimens for each sample were measured by cutting into 1 cm×0.5 cm and the elongation speed was 1 mm/min at standard condition (20 °C, RH 65 ± 5 %).

### Adsorption Capacity Measurement of Metal Ion

The stock solution for metal ion adsorption was prepared by dissolving copper nitrate ($Cu(NO_3)_2$) in 30 mM distilled water. The adsorption capacity in different pH stocks, which were adjusted by adding ammonia water to pH 4.5, 7 and 8.5, was measured for the WK/SF nanofiber mat of 50/50 blend ratio. Before the measurement, to prevent the dissolution of WK in the stock solution, crosslinking was performed with formaldehyde vapor for 24 hours and dried in vacuum oven. The adsorption experiment was carried out by a conventional batch method.

The nanofiber mats were immersed in 10 m*l* stock solution and the vessel containing stock solution was gently shaken for an hour (after equilibrium state). The concentration of Cu (II) ions in stock was measured using an inductively coupled plasma emission spectrometer (ICPS-100IV, Shimadzu, Japan) at wavelength of 327 nm. The amount of adsorbed Cu (II) was calculated based on the difference of Cu (II) ion concentration in the stock solutions before and after adsorption as following equation;

$$\text{Adsorption capacity } (q_e) = \frac{(C_0 - C_e)V}{W}$$

Where, $C_0$ is an initial Cu (II) concentration ($\mu$g/m*l*), $C_e$ is a final Cu (II) concentration ($\mu$g/m*l*), $V$ is a volume of the stock solution (m*l*) and $W$ is a weight of the nanofiber mat (mg).

## Results and Discussion

### Preparation of WK/SF Blend Nanofiber

It is hard to dissolve wool keratin in common solvent due to the cystine crosslinks. Therefore, the disulfide bonds should be broken before preparing the WK dope solution. Using performic acid, the disulfide bonds are broken and cystine residue can be oxidized to cysteic acid without severe chain scission of keratin backbone. Then, the wool keratin is separated into a soluble and insoluble fraction. The insoluble fraction, which had high sulfur content, was very difficult to be dissolved and consequently, this made the electrospinning impossible. On the other hand, the soluble fraction, containing relatively low sulfur content, could be dissolved in formic acid up to 40 % concentration. It has been found that the WK dope solution could be electrospun in the range of 20-40 % concentration but the beads and solution droplets appeared on the nanofiber mats at the

**Table 1.** Electrospinnability of WK/SF blend with various blend ratios and dope concentrations

| Concentration (%) | WK/SF blend ratio | | | | | | |
|---|---|---|---|---|---|---|---|
| | 100/0 | 90/10 | 70/30 | 50/50 | 30/70 | 10/90 | 0/100 |
| 15 | × | ○ | ◎ | ◎ | ◎ | ◎ | ○ |
| 20 | △ | ◎ | ◎ | ◎ | ◎ | × | × |
| 25 | ○ | ◎ | ◎ | × | × | × | × |
| 30 | ○ | ◎ | ◎ | × | × | × | × |
| 35 | ○ | ◎ | × | × | × | × | × |
| 40 | ○ | × | × | × | × | × | × |

×: unable to spin, △: poor; nanofiber was possible to be spun but continuous jet was not maintained, ○: good; wholly stable jet was formed but solution drops often fell down to collector, ◎: excellent; stable drop at the tip end and jet was maintained.

concentration of less than 30 %. The electrospinnability of WK was so poor that stable spinning did not maintain throughout the process due to a low molecular weight (several thousands) of WK solution prepared from soluble fraction of oxidized wool keratin. Furthermore, the electrospun WK nanofiber mats were very brittle to handle and shrunk in aqueous medium. Therefore, the WK nanofiber was hardly used by itself.

To improve the electrospinnability and the end-use properties, WK was blended with SF because the SF is not only easy to electrospin but also has metal ion capacity as protein. At 12 % concentration, the SF exhibited stable electrospinning which make possible to form fine and uniform SF nanofibers. Table 1 shows the electrospinnability of WK/SF blend with various blend ratios and dope concentrations. In most cases, as an increase of SF content ratio, the poor spinnability of WK was complemented and the mean diameter of the blend nanofibers increased in the concentration range of 15-40 %. However, the spinnable range of the dope concentration was narrowed because of high viscosity of SF.

**Structural Characterization of WK/SF Blend Nanofiber**

The morphological structure of the WK/SF blend nanofibers from various conditions were depicted in Figure 1. The nanofiber size increased with SF content and dope concen-

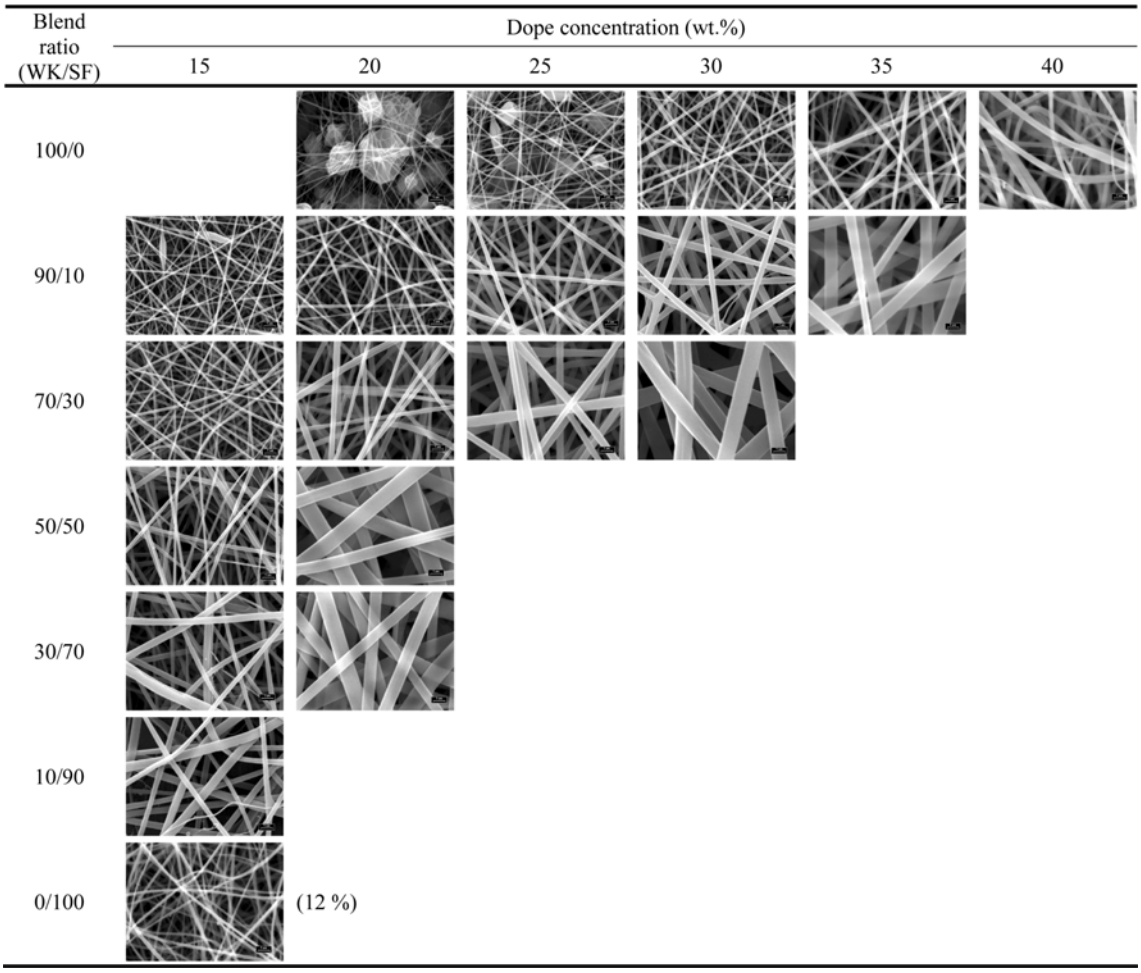


**Figure 1.** SEM micrographs of WK/SF blend nanofibers prepared from various blend ratios and dope concentrations.

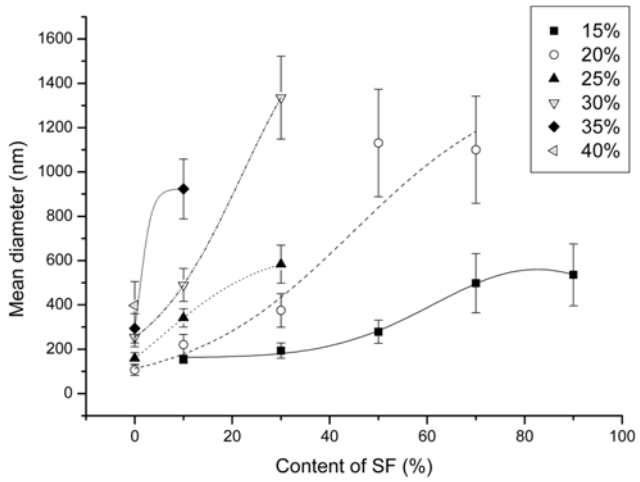


**Figure 2.** Variation in mean diameter of WK/SF blend nanofibers.

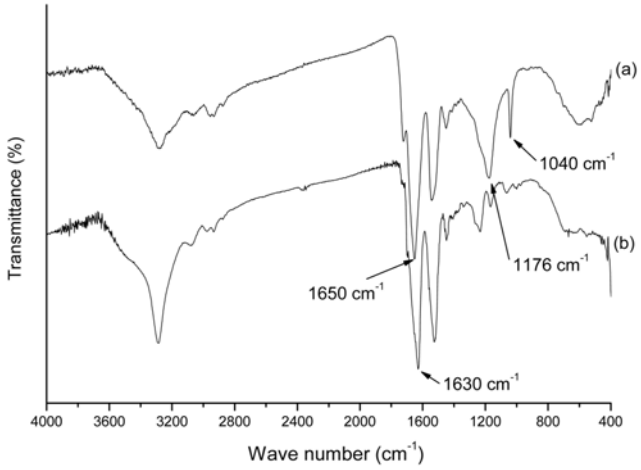


**Figure 3.** FTIR spectra of electrospun (a) WK nanofiber and (b) SF nanofiber.

tration. When the WK content was high and the concentration was low, so-called bead-string shape was observed. On the other hand, an increase of either the SF content or the concentration leaded uniform fiber structure without any beads or drops. In case of the extremely high viscosity of the blend dope, flat type fiber with large band width appeared while the other nanofibers have a circular cross-section in most conditions. Figure 2 shows the effect of SF content and concentration on the mean diameter of the WK/SF blend nanofibers. The higher content of SF and dope concentration, the larger size of nanofiber was obtained. The mean diameter of fiber size was ranged from 100 nm to 1,400 nm. And the change of the fiber size was markedly affected by the concentration especially at a high SF content. This is because the diameter of the WK/SF nanofiber dominantly depends on SF concentration of the blend dope solution rather than WK's concentration due to higher molecular weight of SF.

It has been known that the wool keratin and methanol-treated regenerated SF have $\alpha$-helix and anti-parallel $\beta$-sheet conformation, respectively [27-29]. It was confirmed that the electrospun WK nanofiber had a $\alpha$-helix structure corresponding to the characteristic band of amide I (C=O stretching) and II (N-H deformation and C-N stretching) at 1650 and 1540 $cm^{-1}$, respectively (Figure 3(a)). The figure also showed the bands at 1040 and 1175 $cm^{-1}$ which originated from S=O stretching of cysteic acid [27]. This indicates that the WK soluble fraction used for the electrospinning is one part of the oxidized wool keratin. On the other hand, amide I and II bands appeared at 1630 and 1525 $cm^{-1}$, respectively, for the electrospun SF nanofiber, as shown in Figure 3(b). This corresponds to a $\beta$-sheet conformation of SF [28,29], resulting from the $\beta$-sheet transition by methanol treatment.

Figure 4 show the FTIR spectra of WK/SF blend nanofiber. The amide I and II peaks located at around 1650-1630 $cm^{-1}$ and 1525-1543 $cm^{-1}$, respectively, with different intensities depending on the WK/SF blend ratios. The position of

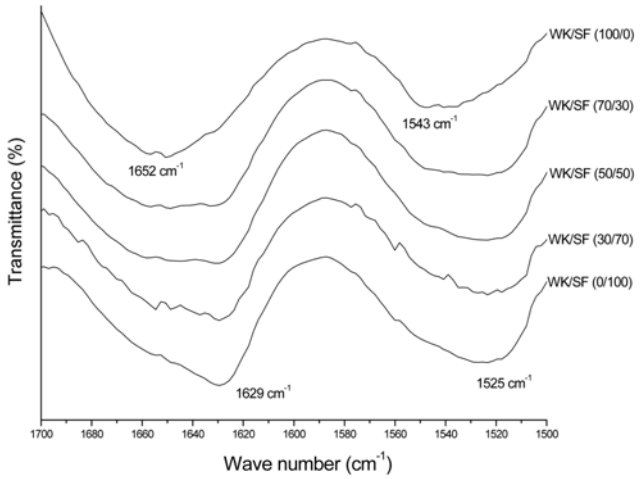


**Figure 4.** FTIR spectra of WK/SF blend nanofibers.

maximum intensity peak of amide I was gradually changed with the content of each component in the WK/SF blend nanofiber. Therefore, it seems no interaction between WK and SF to affect the conformational change by blending because the characteristic bands of $\alpha$-helix and $\beta$-sheet structure appear for the WK/SF blend, respectively.

## Mechanical and Thermomechanical Properties of WK/SF Nanofiber

The mechanical property of the WK/SF blend nanofiber mats was performed by tensile test. Tensile property of membrane, of course, does not directly mean mechanical suitability of water permeable membrane. However, the tensile test is enough to verify the effect of blending on the mechanical behavior of the WK/SF nanofiber mats. Figure 5 shows stress-strain curves of the blend nanofibers with various blend ratios. An initial modulus and breaking stress of WK nanofiber mats were very high while its breaking strain was

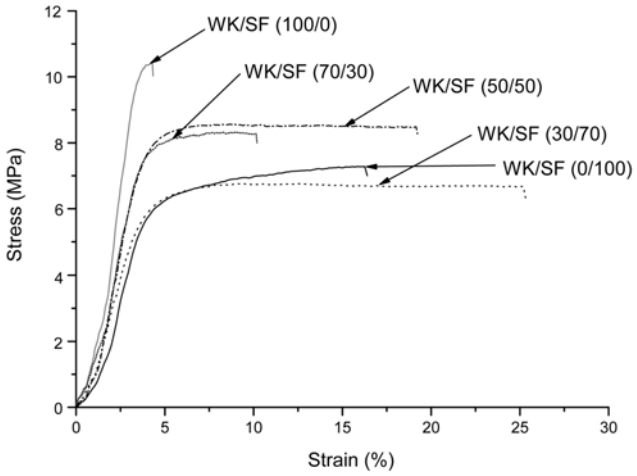


**Figure 5.** Stress-strain curves of WK/SF blend nanofiber mats.

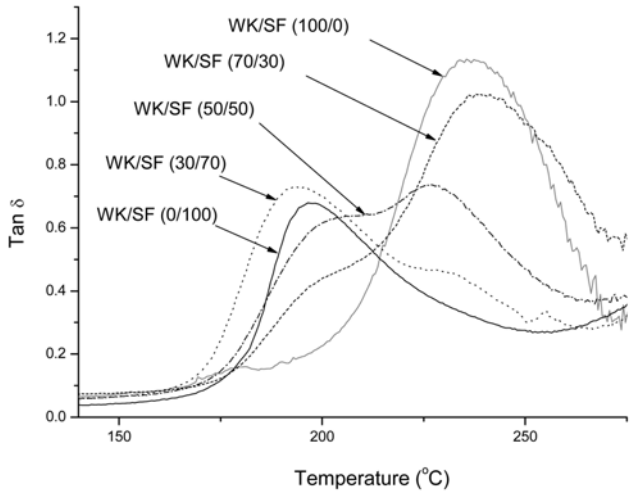


**Figure 6.** Tan$\delta$ of WK/SF blend nanofibers.

very low (4 %), exhibiting a very brittle nature. On the contrary, SF nanofiber mats have a relatively lower breaking stress, higher breaking strain, and higher toughness than WK nanofiber mat. Remarkable point is that WK/SF blend nanofiber mats containing more than 50 % SF content exhibits very high breaking strain. Especially, in the case of 50/50 blend ratio, both breaking stress and strain were significantly improved and compensated, resulting in excellent mechanical property.

Generally, such a synergy effect of mechanical property can be expected in only a miscible blend. Figure 6 shows the DMTA result of the WK/SF blends. In order to find out the miscibility of these blends, WK and SF blend films were cast and used for the DMTA measurement because the nanofiber mats, randomly oriented fiber assembly, can not exactly reflect thermomechanical property. According to the analysis of tan damping peak, glass transition temperature ($T_g$) of WK and SF appeared at 237 and 197 °C, respectively. For all the blends of WK and SF, each characteristic peak was observed only different in maximum intensity of tan$\delta$ peak due to a relative content of each component. This indicates that WK and SF molecules are not miscible in the blend even though morphologically separated domain was not observed in SEM micrograph. But, interesting result was obtained for 50/50 blend ratio of WK/SF. Both tan$\delta$ peaks considerably shifted to a middle temperature, appearing at 227 °C for WK and 202 °C for SF, respectively. Therefore, the miscibility can be improved in 50/50 blend ratio due to possible physical interactions between WK and SF.

Nevertheless, a positive effect was obtained on mechanical property for the WK/SF blend nanofiber mats in spite of phase separation. Of course, it is hard to say the mechanical property of the blend nanofiber mats originated from characteristics of the blend because tensile property must be affected by complicated parameters such as orientation and junction of nanofibers in the nanofiber mats. However, the improvement of breaking strain obtained by blending WK with SF is very positive when the membrane is pressured by permeating water. Therefore, it can be inferred that the blending contributes to applicability of WK/SF blend nanofiber mats as metal ion adsorbent. Considering the mechanical property, adsorption measurement of metal ion was carried out only for 50/50 blend nanofiber mats of WK/SF.

## Adsorption Capacity of $Cu^{2+}$ Metal Ion

Prior to adsorption test, the methanol treated WK/SF blend nanofiber mats were crosslinked by formaldehyde vapor because they were slightly dissolved and shrunk in water due to relatively low molecular weight of WK despite of methanol treatment. However, after crosslinking, the shape of the blend nanofiber mats in water maintained and was not dissolved for a long period. Figure 7 shows the morphological structure of WK/SF (50/50) blend nanofiber mats treated by methanol and crosslinked. As shown in Figure 7(a), the methanol treated nanofiber was swelled and the diameter of the blend nanofiber slightly increased compared with as-spun state (Figure 1). But the fibrous shape was completely destructed after soaking in $Cu^{2+}$ stock solution although the methanol treatment insolublizes SF (Figure 7(b)). On the other hand, the morphological structure of the crosslinked nanofiber showed its fibrous shape maintained after adsorbing $Cu^{2+}$ ions in the stock solution (Figure 7(d)). Here, Figure 7(c) exhibits the morphological structure of methanol treated and subsequently formaldehyde crosslinked WK/SF (50/50) blend nanofiber mats.

Adsorption capacity for $Cu^{2+}$ metal ion was evaluated in different pH conditions because the adsorption is largely affected by charged functional groups of adsorbent with circumstance. Especially, it is very important to evaluate an effect of pH because protein has different charges with pH. Figure 8 shows the effect of pH on $Cu^{2+}$ adsorption capacity of WK/SF (50/50) blend nanofiber mats. The blend nanofiber mats adsorbed more $Cu^{2+}$ at high pH. At pH 8.5, the removal

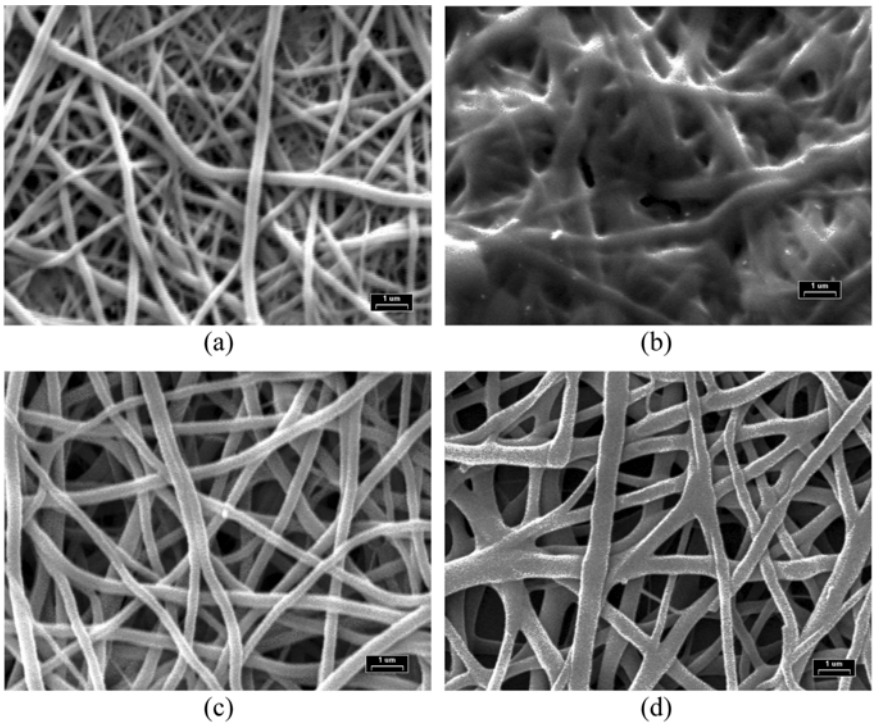


**Figure 7.** SEM micrographs of WK/SF (50/50) blend nanofiber mats. This figure shows the effect of methanol treatment and crosslinking by formaldehyde vapor. (a) and (b) are surface morphology of the mat treated by only methanol before and after soaking in $Cu^{2+}$ stock solution, respectively. (c) and (d) are surface morphology of the mat treated by methanol and subsequently crosslinked by formaldehyde va por before and after soaking in $Cu^{2+}$ stock solution, respectively.

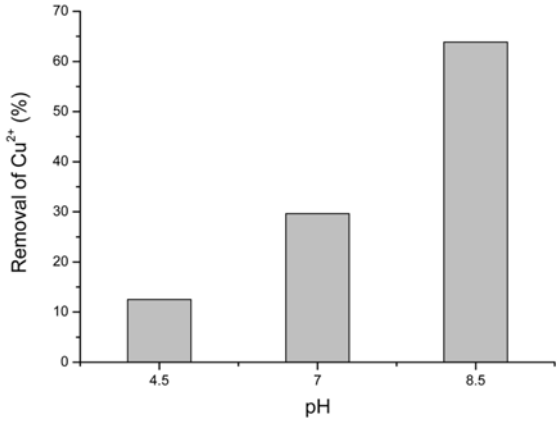


**Figure 8.** The effect of pH on $Cu^{2+}$ adsorption capacity of WK/SF (50/50) blend nanofiber mats.

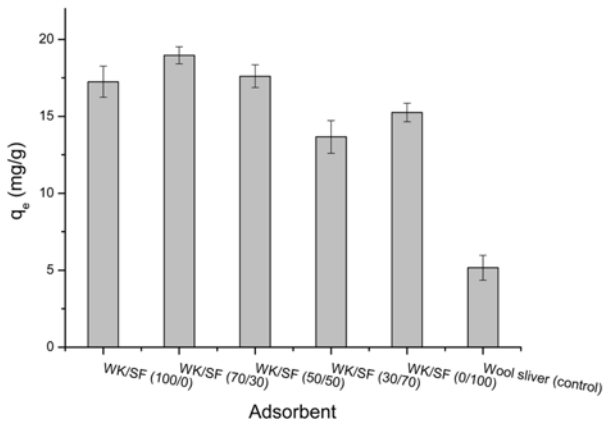


**Figure 9.** $Cu^{2+}$ adsorption capacity of WK/SF blend nanofiber mats of various blend ratios.

value of $Cu^{2+}$ metal ion reached up to 60 % while the value decreased down to 10 % at pH 4.5. In alkaline solution, protein has negatively charged functional groups such as carboxyl groups which can bind with positively charged metal ion. In contrast, in acidic solution, the carboxyl groups lose the negative charge and amine groups have positive charge which repulses metal ions. Therefore, considering that isoelectric point of WK/SF blend is pH 4-5 [30,31], the blend nanofiber mats is efficient as a metal ion adsorbent in solution above pH 5.

As shown in Figure 9, the WK/SF blend nanofiber mats showed an excellent metal ion adsorption capacity regardless of the blend ratio, compared with wool sliver as a control. At same mass, the blend nanofiber mats exhibited three fold capacity of wool sliver. It is mainly due to extremely large surface area of nanofiber. Assuming that the shape of nanofibers is cylinder, the specific areas of the blend nanofiber were in the range of $0.30\times10^{7}$-$3.64\times10^{7}$ $m^{-1}$ while that of the wool sliver was about $0.03\times10^{7}$ $m^{-1}$. Therefore, the nanofiber also

has much more binding sites to metal ion on the surface, reflecting an advantage of nanofiber based on the morphological structure. Merely, the blend nanofiber mats of high WK content adsorbed slightly more $Cu^{2+}$ because WK has more amino acids which have charged side groups and cysteic acid residues than SF. Consequently, it is evident that the WK/SF blend nanofiber can be used for the metal ion adsorbent.

## Conclusion

WK/SF blend nanofiber mat was prepared by electrospinning using soluble fraction of wool keratose and silk fibroin and the effects of various blend ratios and dope concentrations on the electrospinnability and the morphological structure were examined. By blending WK with SF, the electrospinnability was markedly improved and the blend nanofiber has diameters in the range of 100-1,400 nm. The structural and mechanical analysis confirmed phase separation occurred in the WK/SF blends but the miscibility was somewhat improved in the case of 50/50 blend ratio, resulting in an excellent mechanical property such as high breaking stress and strain.

The metal ion adsorption capacity of WK/SF nanofiber mats was investigated with copper ion aqueous solution as a model heavy metal. It was found that $Cu^{2+}$ adsorption occurred more at high pH, being effective above isoelectric point (pH 5) of WK/SF blend. The adsorption capacity was in the range of 14-20 mg/g at pH 8.5 depending on the blend ratio, which was much higher than that of ordinary wool fiber. This is mainly due to large specific surface area of the nanofiber mats as well as many binding sites to metal ions on the WK surface.

## Acknowledgements

The authors of this paper thank the Korea Science and Engineering Foundation (KOSEF) for sponsoring this research through the SRC/ERC Program of MOST/KOSEF (R11-2005-065).

## References

1. P. Kar and M. Misra, *J. Chem. Technol. Biot.*, **79**, 1313 (2004).
2. J. A. Maclaren and B. Miligan, "Wool Science", Science Press, 1981.
3. G. Freddi, T. Arai, G. M. Colonna, A. Boschi, and M. Tsukada, *J. Appl. Polym. Sci.*, **82**, 3513 (2001).
4. M. Dakiky, M. Khamis, A. Manassra, and M. Mer'eb, *Adv. Environ. Res.*, **6**, 533 (2002).
5. P. Taddei, P. Monti, G. Freddi, T. Arai, and M. Tsukada, *J. Mol. Struct.*, **650**, 105 (2003).
6. Y. H. Wang, S. H. Lin, and R. S. Juang, *J. Hazard. Mater.*, **102**, 291 (2003).
7. H. S. Park and Y. O. Park, *Korean J. Chem. Eng.*, **22**, 165 (2005).
8. X. F. Wang, X. M. Chen, K. Yoon, D. F. Fang, B. S. Hsiao, and B. Chu, *Environ. Sci. Technol.*, **39**, 7684 (2005).
9. C. Kim and K. S. Yang, *Appl. Phys. Lett.*, **83**, 1216 (2003).
10. J. Zeng, X. Xu, X. Chen, Q. Liang, X. Bian, L. Yang, and X. Jing, *J. Control. Release*, **92**, 227 (2003).
11. E. R. Kenawy, G. L. Bowlin, K. Mansfield, J. Layman, D. G. Simpson, E. H. Sanders, and G. E. Wnek, *J. Control. Release*, **81**, 57 (2002).
12. W. J. Li, C. T. Laurencin, E. J. Caterson, R. S. Tuan, and F. K. Ko, *J. Biomed. Mater. Res. A*, **60**, 613 (2002).
13. K. Kim, M. Yu, X. H. Zong, J. Chiu, D. F. Fang, Y. S. Seo, B. S. Hsiao, B. Chu, and M. Hadjiargyrou, *Biomaterials*, **24**, 4977 (2003).
14. W. J. Li, R. Tuli, X. X. Huang, P. Laquerriere, and R. S. Tuan, *Biomaterials*, **26**, 5158 (2005).
15. S. A. Riboldi, M. Sampaolesi, P. Neuenschwander, G. Cossu, and S. Mantero, *Biomaterials*, **26**, 4606 (2005).
16. K. N. Chua, W. S. Lim, P. Zhang, H. Lu, J. Wen, S. Ramakrishna, K. W. Leong, and H. Q. Mao, *Biomaterials*, **26**, 2537 (2005).
17. B. Ding, J. Kim, Y. Miyazaki, and S. Shiratori, *Sensor. Actuat. B-Chem.*, **101**, 373 (2004).
18. X. Wang, C. Drew, S. H. Lee, K. J. Senecal, J. Kumar, and L. A. Samuelson, *Nano Lett.*, **2**, 1273 (2002).
19. X. Wang, Y. G. Kim, C. Drew, B. C. Ku, J. Kumar, and L. A. Samuelson, *Nano Lett.*, **4**, 331 (2004).
20. H. F. Jia, G. Y. Zhu, B. Vugrinovich, W. Kataphinan, D. H. Reneker, and P. Wang, *Biotechnol. Progr.*, **18**, 1027 (2002).
21. K. H. Lee, C. S. Ki, D. H. Baek, G. D. Kang, D. W. Ihm, and Y. H. Park, *Fibers and Polymers*, **6**, 181 (2005).
22. H. Wang, Y. P. Zhang, H. L. Shao, and X. C. Hu, *J. Mater. Sci.*, **40**, 5359 (2005).
23. M. Wang, H. J. Jin, D. L. Kaplan, and G. C. Rutledge, *Macromolecules*, **37**, 6856 (2004).
24. K. Ohgo, C. Zhao, M. Kobayashi, and T. Asakura, *Polymer*, **44**, 841 (2003).
25. T. Arai, G. Freddi, G. M. Colonna, E. Scotti, A. Boschi, R. Murakami, and M. Tsukada, *J. Appl. Polym. Sci.*, **80**, 297 (2001).
26. P. Taddei, P. Monti, G. Freddi, T. Arai, and M. Tsukada, *J. Mol. Struct.*, **651**, 433 (2003).
27. J. Koga, K. Kawaguchi, E. Nishio, K. Joko, N. Ikuta, I. Abe, and T. Hirashima, *J. Appl. Polym. Sci.*, **37**, 2131 (1989).
28. I. C. Um, H. Y. Kweon, K. G. Lee, and Y. H. Park, *Int. J. Biol. Macromol.*, **33**, 203 (2003).
29. H. J. Jin, S. V. Fridrikh, G. C. Rutledge, and D. L. Kaplan, *Biomacromolecules*, **3**, 1233 (2002).
30. C. Wong Po Foo, E. Bini, J. Hensman, D. P. Knight, R. V. Lewis, and D. L. Kaplan, *Appl. Phys. A*, **82**, 223 (2006).
31. H. J. An, MS Thesis, Seoul National University, Seoul, Republic of Korea, 1997.